Strong interseismic coupling, fault afterslip, and viscoelastic flow before and after the Oct. 9, 1995 Colima-Jalisco earthquake: Continuous GPS measurements from Colima, Mexico

Bertha Márquez Azúa
Universidad de Guadalajara, Guadalajara, Jalisco, Mexico

Charles DeMets
Department of Geology and Geophysics, UW-Madison, Madison, Wisconsin, USA

Tim Masterlark
U.S. Geological Survey, EROS Data Center, Raytheon, Sioux Falls, South Dakota, USA

Received 10 January 2002; revised 12 February 2002; accepted 14 February 2002; published 30 April 2002.

[1] Continuous GPS measurements from Colima, Mexico during 4/93–6/01, bracketing the Oct. 9, 1995 M = 8.0 Colima-Jalisco earthquake, provide new constraints on Rivera plate subduction mechanics. Modeling of margin-normal strain accumulation before the earthquake suggests the Rivera-North America subduction interface was fully locked. Transient postseismic motion from 10/95–6/97 is well fit by a model that includes logarithmically-decaying fault afterslip, elastic strain from shallow fault relocking, and possibly a minor viscoelastic response, but is fit poorly by models that assume a dominant Maxwell viscoelastic response of the lower crust and upper mantle, independent of the assumed viscosities. Landward, margin-normal motion since mid-1997 is parallel to but ~75% slower than the pre-seismic velocity. Afterslip alone fails to account for this slowdown. The viscoelastic response predicted by a FEM correctly resolves the remaining velocity difference within the uncertainties. Both processes thus offset elastic strain accumulating from the relocked subduction interface. *INDEX TERMS:* 1208 Geodesy and Gravity: Crustal movements—intraplate (8110); 1242 Geodesy and Gravity: Seismic deformations (7205); 7209 Seismology: Earthquake dynamics and mechanics; 8123 Tectonophysics: Dynamics, seismotectonics

1. Introduction

[2] The M_w = 8.0 October 9, 1995 Colima-Jalisco earthquake ruptured a ~150-km-long segment of the northernmost Middle America trench that had been seismically quiescent since 1932. Modeling of teleseismic waveforms [*Mendoza and Hartzell*, 1999] and GPS displacements at 11 sites near the rupture zone [*Melbourne et al.*, 1997; *Hutton et al.*, 2001] suggest that up to five meters of coseismic slip occurred in two principal patches, both above depths of 20 km (Figure 1). Geodetically-measured displacements during a 3.5-year period following the earthquake suggest that the earthquake triggered afterslip below depths of 20 km and along parts of the subduction interface southeast of the main rupture zone [*Hutton et al.*, 2001], presumably representing localized shear along velocity-strengthening regions of the subduction interface.

0094-8276/02/2002GL014702$05.00

[3] Here, we use previously unavailable data from a continuously operating GPS station (COLI) in Colima, Mexico to study the dynamics of subduction in this region and elsewhere. The new data, which greatly exceed the temporal resolution of pre-existing geodetic measurements [*Melbourne et al.*, 1997; *Hutton et al.*, 2001] and span an eight-year period (4/93–6/01) that brackets the Colima Jalisco earthquake, afford a unique view of the seismic cycle for this subduction zone and provide new information about the postseismic effects of fault afterslip, viscous flow of the lower crust and upper mantle, and elastic strain due to fault relocking. Elastic half-space and finite-element modeling (FEM) of the new data reveals, for the first time, the degree of pre-seismic locking and a significant linear component in the postseismic deformation likely caused by a combination of a viscoelastic response and relocking of the subduction interface. They also confirm previously reported evidence for afterslip [*Hutton et al.*, 2001].

2. Data and Analysis

[4] The GPS data we use were collected by the Mexican government agency INEGI between April, 1993 and mid-2001 with an L1/L2, C/A code receiver. Due to logistical limitations, we procured only one 24-hour session per week, except for a 10-month period bracketing the Colima-Jalisco earthquake, for which we procured daily GPS sessions. Prior to 1/22/96, the GPS antenna was located on the roof of an older building in the city of Colima, after which it was moved to the roof of a modern nearby building. No geodetic site tie was made between the two sites. We thus link the two coordinate time series in a manner that optimizes their continuity.

[5] We analyzed the GPS data using GIPSY, satellite orbits and clocks from the Jet Propulsion Laboratory, and a standard point-positioning strategy [*Zumberge et al.*, 1997]. Daily free-network station coordinates were transformed to ITRF97 [*Boucher et al.*, 1999], yielding 3D coordinate time series. Motion of the North American plate relative to ITRF97, derived from the velocities of 140 GPS stations in the plate interior for which daily data are analysed at the University of Wisconsin, was removed from the time series so as to recast site motion relative to North America (Figure 2). Daily white noise in the north, east, and vertical components (4 mm, 7 mm, and 11 mm) is comparable to noise reported for many other continuous GPS sites [*Zumberge et al.*, 1997], as is the long-period noise. All velocity and displacement uncertainties quoted herein are 1σ and are estimated using a model

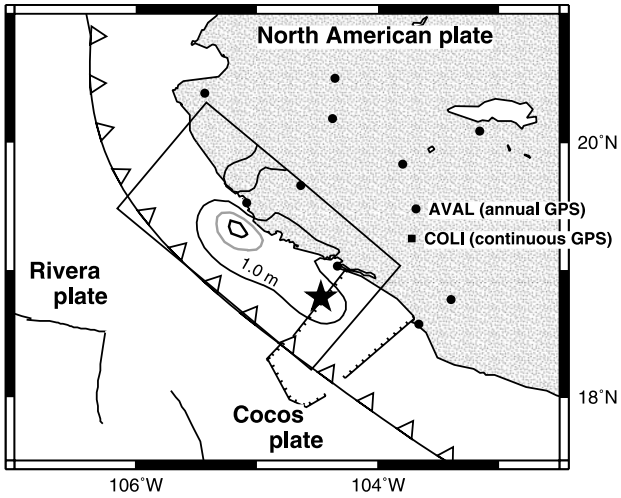

Figure 1. Upper—Tectonic setting and coseismic slip distribution from *Hutton et al.* [2001]. Rectangle shows surface projection of fault used for elastic half-space and viscoelastic modeling. Contours show coseismic downdip slip, ranging from 1 meter to 5 meters (bold line). Star shows epicenter of Oct. 9, 1995 Colima-Jalisco earthquake. Circles show locations of GPS sites used to constrain coseismic slip distribution.

for white- and time-correlated noise in GPS coordinate time series [*Mao et al.*, 1999].

3. Modeling and Assumptions

[6] Our interpretation of the data is guided by modeling of rectangular dislocations in an elastic half-space [*Okada*, 1985] and finite-element modeling (FEM) of the viscoelastic and poroelastic responses to the Colima-Jalisco earthquake. The laterally and vertically heterogeneous FEM we use to predict postseismic surface deformation consists of a curved subduction interface that separates oceanic from continental lithosphere. It is identical to the FEM_C model of *Masterlark et al.* [2001], with the addition of viscous flow in the mantle. We divide continental lithosphere into a poroelastic upper crust and a Maxwell viscoelastic lower crust and upper mantle, with assumed respective viscosities of 5×10^{18} Pa sec and 1×10^{19} Pa sec [*Masterlark*, 2000; *Wang et al.*, 2001]. Viscoelastic flow within the lower two layers, representing solid-state creep processes that occur in response to coseismic stress jumps, induces two superimposed, exponentially-decaying deformations at the surface. *Hutton et al.* [2001] describe the subduction interface that optimizes the fit to coseismic and postseismic GPS displacements associated with the Colima-Jalisco earthquake. *Masterlark et al.* [2001] describe the FEM geometry, elastic properties, and technique we use to predict the time-dependent poroelastic and viscoelastic surface responses.

[7] Forward calculations of the approximate viscoelastic response from the June 3 and June 18, 1932 Jalisco earthquakes, with estimated magnitudes of M = 8.2 and M = 7.8 [*Singh et al.*, 1985], predict maximum present-day displacements at COLI slower than 1 mm yr^{-1} toward the west and south. The small, residual viscoelastic effects of these earthquakes are ignored below.

4. Results and Discussion

4.1. Interseismic Strain: 4/1993–10/9/1995

[8] GPS measurements at COLI during 4/93–10/95 provide the only known constraints on the rate and direction of surface deformation preceding the Colima-Jalisco earthquake. A linear best-fit to the coordinate time series for this period (Figure 2) gives a velocity of 10 ± 2.5 mm yr^{-1} toward N46°E ± 12°, representing margin-normal shortening with respect to the plate interior. Assuming this represents elastic strain accumulating in response to unrelieved plate slip along the Rivera-North America and Cocos-North America subduction interfaces, we predicted the velocity at COLI from a uniform elastic half-space model within which geometrically realistic Rivera and Cocos plate subduction interfaces are embedded and fully locked to depths of 25 km. Location-dependent convergence rates and directions along the subduction interfaces are specified by the 0.78 Ma-average Rivera-North America and Cocos-North America angular velocities of *DeMets and Wilson* [1997]. The elastic half-space model predicts motion at COLI of 9 mm yr^{-1} toward N38°E. Motion predicted by the heterogeneous FEM is nearly identical.

[9] Provided that the GPS monument at COLI was stable during the years before the earthquake and the plate kinematic model we employ is accurate, the good agreement between the observed and predicted interseismic velocities (Figure 2) implies that the shallow regions of the Rivera-North America subduction interface were fully locked prior to the Colima-Jalisco earthquake.

4.2. Coseismic Motion: October 9 1995

[10] The coseismic displacement, 132 mm toward S66°W (Figure 2), is determined from the difference in the site coordinates predicted for October 9, 1995 by the linear-change model for motion before the earthquake (see previous section) and a linear/logarithmic decay model for transient postseismic motion (see below). Relative to the coseismic displacement at COLI, coseismic motion at nearby GPS site AVAL (Figure 1) is ∼15% greater and points toward the southwest (Figure 2). As described in the next section, the difference in the coseismic displacements of the two sites agrees well with results reported by *Hutton et al.* [2001].

4.3. Transient Postseismic Motion

[11] Motion during the twenty month period following the earthquake (Figure 2) decayed rapidly and was dominated by SSW-directed displacement 44° counterclockwise (CCW) from the coseismic direction. The predicted poroelastic response at COLI is too small [*Masterlark et al.*, 2001] to explain the decaying displacement. Similarly, the viscoelastic response predicted by a FEM in which the upper mantle and lower crust are loaded by the well-constrained distribution of coseismic displacement is too small and in the wrong direction (Figure 2). The poor fit persists for a wide range of viscosities for the lower crust and upper mantle (1×10^{17} Pa sec to 1×10^{20} Pa sec), as well as for models with non-linear and hence time-dependent upper mantle viscosity [*Pollitz et al.*, 2001]. We conclude that poroelastic and Maxwell viscoelastic responses to the earthquake cannot explain the majority of the transient deformation during this period.

[12] An alternative explanation is that friction along the subduction interface is governed by rate- and state-variable constitutive laws, in which case any afterslip along the subduction interface and hence displacements at the surface will decay logarithmically [e.g. *Scholz*, 1990]. To test this, we fit $u(t) = d + A * \ln(bt + 1)$ to the north and east displacement components $u(t)$ for times before mid-1997 while requiring a common decay constant b and separate values of d and A for the north and east components. Optimizing the least-squares fit yields good fits to both components for times before mid-1997, but mis-predicts displacements after mid-1997 (Figure 2). We also tested a model that includes logarithmic decay and a linear displacement component, the later presumably resulting from a combination of linearly accumulating strain due to a relocked subduction interface and slowly decaying and thus nearly linear viscoelastic rebound. The least-squares fit of the combined model improves on the fit of the simpler logarithmic decay model at much more than the 99% confidence level. The observations prior to mid-1997 thus contain useful information about the

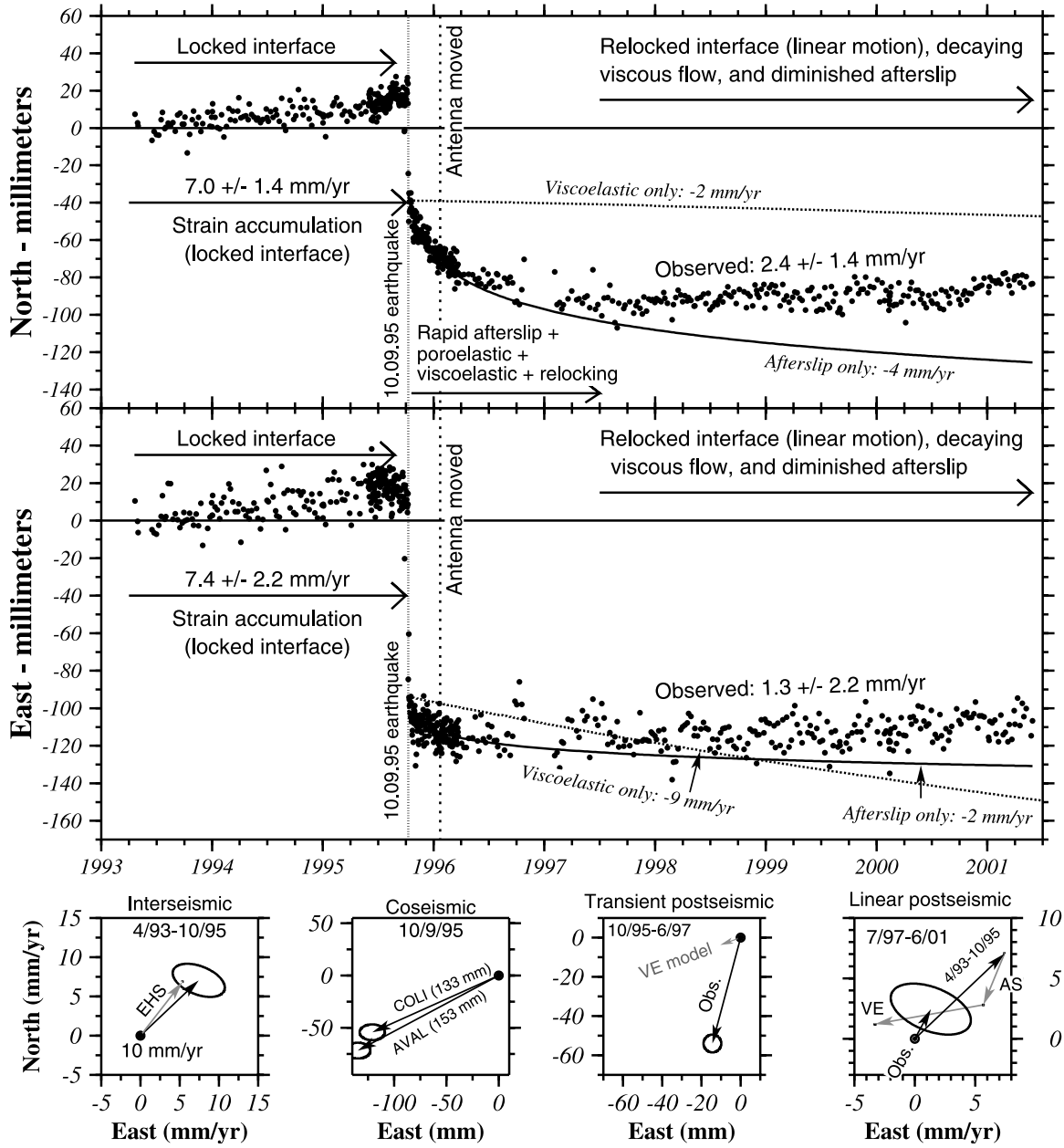

Figure 2. GPS coordinate time series for COLI relative to North American plate. Dashed line denotes when the GPS monument was moved to a nearby building (see text). Dotted line shows viscoelastic displacements predicted by a finite-element model driven by coseismic fault slip. The four lower panels summarize displacements for the interseismic (pre-seismic), coseismic, and two postseismic intervals. The coseismic displacement measured at a nearby GPS site AVAL (location shown in Figure 1) includes 11 days of slip following the Oct. 9, 1995 earthquake [*Hutton et al.*, 2001]. The interseismic velocity predicted by a fully-coupled elastic-half space model is labeled "EHS". Viscoelastic and afterslip model predictions are labeled "VE" and "AS" respectively. Rightmost panel shows the observed postseismic velocity for the interval 7/97–6/01 (Obs.), velocities predicted by viscoelastic and afterslip models, and the interseismic velocity from the leftmost subpanel. All uncertainties are 1σ.

logarithmic decay parameters and a linear term. The latter has not been previously detected for this earthquake.

[13] These results are consistent with observations and predictions described in *Hutton et al.* [2001]. The CCW rotation of the direction of postseismic motion at COLI (Figure 2) mirrors similar CCW rotations observed at AVAL and other GPS sites. Modeling by *Hutton et al.* [2001] suggests this rotation is best interpreted as evidence that most afterslip was focused southeast and downdip from the principal earthquake rupture zone. In addition, the cumulative postseismic displacement at COLI ten days after the earthquake is observed to be ~15% of the coseismic displacement (Figure 2), consistent with a ~15–25% estimate predicted by *Hutton et al.* [2001] from extrapolation of their measured postseismic GPS displacements back to the time of the earthquake.

4.4. Linear Postseismic Motion: 7/1997–5/2001

[14] Since mid-1997, COLI has moved 2.8 ± 1.2 mm yr^{-1} toward N29°E ± 5° (Figure 2), nearly parallel to but ~75% slower than the rate of margin-normal shortening before the earthquake. Although the decreased rate of surface displacement could repre-

sent a temporary or possibly permanent decrease in the degree of locking along the subduction interface, we argue below that motion since mid-1997 more likely represents linearly accumulating elastic strain due to a fully relocked subduction interface, offset by the effects of continued fault afterslip and viscous flow in the lower crust and upper mantle.

[15] If we assume that the velocity since mid-1997 will eventually return to the pre-earthquake velocity upon sufficient decay of afterslip and any viscous flow, the present velocity difference between the two (lower right panel, Figure 2) presumably represents the net surface response to continued fault afterslip and viscous flow. Afterslip predicted by the logarithmic-decay and linear-motion model (Figure 2) is in the wrong direction and too slow to account for the observed difference between the pre-seismic velocity and the velocity since mid-1997. Encouragingly, the viscoelastic response since mid-1997 predicted by the FEM points in the correct direction needed to resolve the remaining velocity difference (Figure 2). Although the predicted viscoelastic response is too large by roughly a factor of two, its magnitude can be reduced by a factor of two by increasing the assumed viscosity of the lower crust to a slightly higher value of 1×10^{19} Pa sec. We did not fine tune the viscosity structure to optimize the fit because our simplified modeling approach ignores coupling between afterslip and viscous flow, and because the problem is generally underdetermined.

[16] Better estimates of the relative contributions of strain accumulation, afterslip, and viscous flow will require more data, simultaneous modeling of the coupled viscoelastic and afterslip responses, improved estimates of the viscosity structure at depth, and consideration of alternative models for viscous flow (e.g. Maxwell, power-law creep, anisotropic). We are presently modeling the displacements of ~20 additional GPS sites in this region toward this goal.

[17] **Acknowledgments.** This work is funded by NSF grant EAR-9804905 and is additionally supported by the University of Guadalajara, University of Wisconsin, and INEGI. We thank Geoff Blewitt and Ralph Glaus for developing procedures to utilize C/A code and L1/L2 phase measurements for precise point positioning, Kristine Larson and two anonymous reviewers for constructive comments, Wallis Hutton for assistance at the beginning of this project, and the JPL/IGS analysis center for precise satellite orbits.

References

Boucher, C., Z. Altamimi, and P. Sillard, The 1997 International Terrestrial Reference Frame (ITRF97), *IERS Technical Note*, *27*, 1999.

DeMets, C., and D. S. Wilson, Relative motions of the Pacific, Rivera, North American, and Cocos plates since 0.78 Ma, *J. Geophys. Res.*, *102*, 2789–2806, 1997.

Hutton, W., C. DeMets, O. Sanchez, G. Suarez, and J. Stock, Slip kinematics and dynamics during and after the 1995 October 9 M_w = 8.0 Colima-Jalisco earthquake, Mexico, from GPS geodetic constraints, *Geophys. J. Int.*, *146*, 637–658, 2001.

Mao, A., C. G. A. Harrison, and T. H. Dixon, Noise in GPS coordinate time series, *J. Geophys. Res.*, *104*, 2797–2816, 1999.

Masterlark, T., Regional fault mechanics following the 1992 Landers earthquake, Ph.D. thesis, 83 pp., University of Wisconsin-Madison, Madison, Wisconsin, 2000.

Masterlark, T., C. DeMets, H. Wang, O. Sanchez, and J. Stock, Homogeneous vs heterogeneous subduction zone models: Coseismic and post-seismic deformation, *Geophys. Res. Lett.*, in press, 2001.

Melbourne, T., I. Carmichael, C. DeMets, K. Hudnut, O. Sanchez, J. Stock, G. Suarez, and F. Webb, The geodetic signature of the *M* 8.0 October 9, 1995, Jalisco subduction earthquake, *Geophys. Res. Lett.*, *24*, 715–718, 1997.

Mendoza, C., and S. Hartzell, Fault-slip distribution of the 1995 Colima-Jalisco, Mexico, earthquake, *Bull. Seismol. Soc. Am.*, *89*, 1338–1344, 1999.

Okada, Y., Surface deformation due to shear and tensile faults in a half-space, *Bull. Seismol. Soc. Am.*, *75*, 1135–1154, 1985.

Pacheco, J. F., L. R. Sykes, and C. H. Scholz, Nature of seismic coupling along simple plate boundaries of the subduction type, *J. Geophys. Res.*, *98*, 14,133–14,159, 1993.

Pollitz, F. F., C. Wicks, and W. Thatcher, Mantle flow beneath a continental strike-slip fault: Postseismic deformation after the 1999 Hector Mine earthquake, *Science*, *293*, 1814–1818, 2001.

Scholz, C. H., *The mechanics of earthquakes and faulting*, Cambridge University Press, Cambridge, 1990.

Singh, S. K., L. Ponce, and S. P. Nishenko, The great Jalisco, Mexico, earthquakes of 1932: Subduction of the Rivera plate, *Bull. Seismol. Soc. Am.*, *75*, 1301–1313, 1985.

Wang, K., J. He, H. Dragert, and T. S. James, Three-dimensional viscoelastic interseismic deformation model for the Cascadia subduction zone, *Earth, Planets, and Space*, *53*, 295–306, 2001.

Zumberge, J. F., M. B. Heflin, D. C. Jefferson, M. M. Watkins, and F. H. Webb, Precise point positioning for the efficient and robust analysis of GPS data from large networks, *J. Geophys. Res.*, *102*, 5005–5017, 1997.

B. Márquez Azúa, Department de Geografía y Ordenación Territorial, Universidad de Guadalajara, Av. de los Maestros y Mariano Barcena. Planta Alta, Guadalajara, Jalisco, México. (bmarquez@udgserv.cencar.udg.mx)

C. DeMets, Department of Geology and Geophysics, UW-Madison, 1215 W Dayton St., Madison, WI 53706, USA. (chuck@geology.wisc.edu)

T. Masterlark, Raytheon ITSS Corporation USGS/EROS Data Center, 47914 252nd St., Sioux Falls, SD 57198, USA. (master@usgs.gov)